

Nonlocality Induces Chains of Nested Localized Structures

J. Javaloyes,¹ M. Marconi,² and M. Giudici²

¹*Departament de Física, Universitat de les Illes Balears, C/Valldemossa km 7.5, 07122 Mallorca, Spain*

²*Université Côte d'Azur, CNRS, Institut de Physique de Nice, F-06560 Valbonne, France*

Localized Structures often behave as quasi-particles and they may form molecules characterized by well-defined bond distances. In this paper we show that pointwise nonlocality may lead to a new kind of molecule where bonds are not rigid. The elements of this molecule can shift mutually one with respect to the others while remaining linked together, in a way similar to interlaced rings in a chain. We report experimental observations of these chains of nested localized structures in a time-delayed laser system.

PACS numbers: 42.65.Sf, 02.30.Ks, 05.45.-a, 89.75.Fb

In a seminal contribution, Alan Turing set the bases of morphogenesis [1]. He demonstrated that, in a dissipative environment, the interplay between *local* nonlinearities and differential operators was sufficient to initiate self-organization and generate an infinite variety of patterns. These emergent structures can be found in many physical, biological, and laboratory systems. Among them, localized structures (LSs) are of particular interest and have been widely observed in nature [2–6]. These states can be individually addressed by a local perturbation, without affecting their surrounding environment. They are particularly relevant for applications when implemented in optical resonators as light bits for information processing [7–15]. Localized Structures may form bound states, also called “molecules”, via the overlap of their oscillating tails which creates “covalent” bonds corresponding to stable equilibrium distances [6, 16, 17].

In this letter we disclose a different kind of molecule composed by chains of nested LSs, which are globally bounded yet locally independent, and similar to an ensemble of interlaced rings. Interesting enough, similar molecular structures exist in chemistry. They are composed by interlocked macrocycles and they are called catenanes [18]. While usual covalent bound states of LSs move as a rigid ensemble when subject to perturbations, the stability analysis of these interlaced LSs reveals that they exhibit several neutral modes corresponding to the individual translation of each element. In other words, small displacements between the components do not relax, yet the ensemble remains stable. We show that these molecules, which challenge the usual notion of local stability for LS compounds, can be obtained in presence of a pointwise nonlocality coupling a field $\Phi(x, t)$ to a distant point in space $\Phi(x + a, t)$.

Nonlocality has been widely explored in spatially extended systems and has been shown to induce patterns [19], convective instabilities [20, 21] or N-fold structures [22]. Distributed nonlocality was recently found capable of stabilizing LSs [23] and identified as an important mechanism governing the morphogenesis processes in liquid crystal [24] and vegetation patterns [25]. Global coupling, as an extreme case of nonlocality, is known to have a deep impact on LSs bifurcation diagrams [26].

The difference between standard covalent molecules and the nested states is illustrated in the qualitative sketches of Fig. 1. We represent in Fig. 1(a) an elementary LS solution stemming from a generic partial differential equation (PDE) able to sustain LSs in one spatial dimension (x). The characteristic length of the LS is denoted l . A small pointwise nonlocal perturbation can be modeled for instance as a linear perturbation of a PDE that reads

$$\partial_t \Phi = \mathcal{F}(|\Phi|^2, \partial_x^2) \Phi + \varepsilon \Phi(x + a, t) \quad (1)$$

with \mathcal{F} an operator representing e.g. the Ginzburg-Landau equation as in [27, 28]. Without loss of generality we assume $a > 0$. For sufficiently small ε , the overall structure of the original LS remains preserved, but it develops a small echo of amplitude ε at the distance a , as a consequence of the nonlocal term. Additional weaker replica of this echo also appear at distances na ($n \in \mathbb{N}$) with amplitudes ε^n , but they can be neglected in this discussion. If $\varepsilon = 0$, standard covalent molecules can be generated by the interaction between the decaying oscillating tails of two nearby LSs. This leads to equilibrium distances $d \sim l$ (not shown). When $\varepsilon \neq 0$, and for moderate nonlocality $a \sim l$, the rightmost LS tail will be modified, which may lead to additional equilibrium distances that persist even when $a \gg l$. Here the binding occurs as a consequence of the interaction between the main pulse of a second LS and the echo of the first, leading to an equilibrium distance $d \sim a$, see Fig. 1(b). All these rigid molecules feature well-determined bond

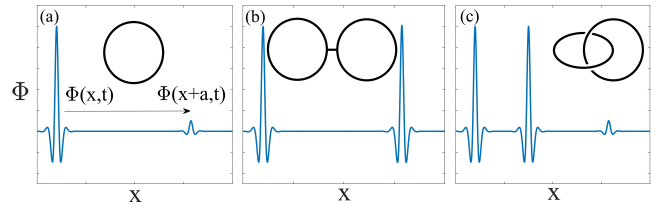


Figure 1. (a) Sketch of a LS with a pointwise nonlocal term where the field $\Phi(x, t)$ induces a perturbation at a distance a . (b) Covalent molecule where bonding occurs via tail interactions. (c) Molecule with a nested element.

lengths and a single neutral mode corresponding to the translation degree of freedom of the whole ensemble. A novel kind of molecule appears in the case $a \gg l$, when the second LS is placed at a distance d from the first LS such that $l < d < a$. In this case, shown in Fig. 1(c), the two LSs are sufficiently far so that they can move independently but, at the same time, the second LS cannot overcome the repulsive barrier induced by the echo of the first LS. As such, the two LSs are globally linked while being locally independent. A useful analogy to picture these situations can be made using rings which are rigidly bounded in the situation represented in Fig. 1(b), while they are interlaced in the case of Fig. 1(c).

Pointwise nonlocality may not be easy to achieve experimentally and, in order to observe such new bounded states, we have studied their realization in a time-delayed system (TDS). In recent years, building on the strong analogies between spatially extended and time-delayed systems [29–31], the latter have been proposed for controlling spatial LSs [32], hosting chimera states [33], domain walls [34–37], vortices [38] and, in particular, temporal LSs [39–43], see [44] for a review. The idea that a time delay τ is akin to a spatial dimension is rooted in the representation developed in [29] that consists in cutting a single temporal time trace generated by a TDS into $n \in \mathbb{N}$ chunks of duration T (with $T \simeq \tau$) and stack them into a two dimensional map. The horizontal dimension plays the role of a pseudo-spatial variable representing the profile of the pulse within the n -th period while the vertical axis depicts the discrete time index n . In some situations [30], this two-dimensional representation can even lead to an analytical description of a TDS as a PDE containing *local* operators, as e.g. Laplacian. In this formalism, the temporal profile over one period—the information in pseudo-space—is mapped onto the next period. As such, one understands that the inclusion of a second delay $\tau_2 = a$ induces a pointwise nonlocality coupling each point of the temporal profile to itself, but with a shift a . In addition, similar results are to be found for $\tau_2 = pT + a$ if $p \in \mathbb{N}$ is sufficiently small so that the temporal profile does not evolve much during p periods.

An example of a photonic system with a double time delay capable of hosting LSs and molecules has been recently described [42] and is summarized in Fig. 2(a). A single-transverse mode vertical-cavity surface-emitting laser (VCSEL) is coupled to an external cavity that selects one of the linearly polarized states of the VCSEL (Y, say) and feeds it back twice, once with a time delay τ_f , and once with a delay τ_r after being rotated into the orthogonal direction. When τ_f is much larger than the laser timescales and for properly chosen parameters, this system hosts vectorial LSs which correspond to a full rotation of the polarization vector state on the Poincaré sphere. Along the X polarization component, they correspond to upward pulses over a low intensity background while they correspond to anti-phase downward pulses in the Y polarization component, see Fig. 2(b,c). The situation depicted in Fig. 2(a) is well described by the so-

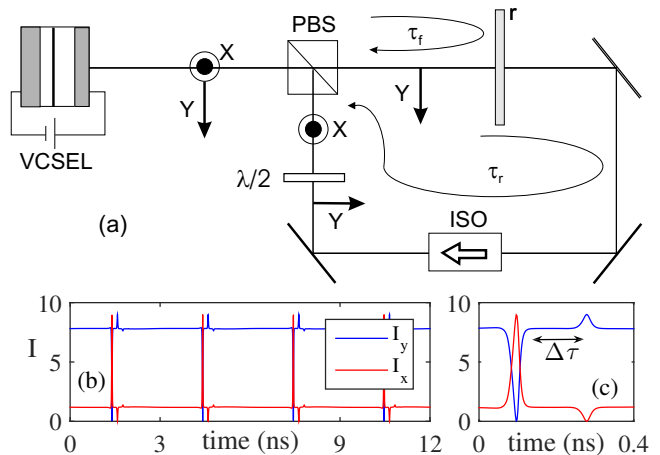


Figure 2. (a) Experimental setup. The polarizing beam splitter (PBS) splits the X and Y components of the field. r is a partially reflective mirror that feeds back the Y component after a time of flight τ_f . The optical isolator (ISO) only allows for the transmission of the field traveling from right to left. The half waveplate ($\lambda/2$) rotates the transmitted Y component of the field into its orthogonal polarization, which is then re-injected after a time delay τ_r . (b,c) Numerical integration of Eq. (2). Temporal trace corresponding to a periodic regime with a single LS (b) and (c) close-up around the LS ($\Delta\tau = \tau_r - \tau_f$).

called Spin-Flip Model [45] supplemented by the inclusion of the delayed re-injection terms. Yet, a multiple timescales analysis of this model applied in the limit of large damping of the relaxation oscillations, weak dichroism γ_a , moderate birefringence γ_p and feedback rates (η, β) leads to a decoupling between the equations for the total intensity I_0 , the population inversion, the field ellipticity and the optical phase, from the equation describing the polarization vector longitude Φ along the equatorial plane of the Poincaré sphere [46]. The following simpler delayed equation was found to reproduce well the dynamics,

$$\dot{\Phi} = z \sin \Phi + \bar{\eta} \sin \frac{\Phi \tau_f}{2} \cos \frac{\Phi}{2} - \bar{\beta} \sin \frac{\Phi}{2} \sin \frac{\Phi \tau_r}{2}, \quad (2)$$

with $\Phi^{\tau_{f,r}} = \Phi(t - \tau_{f,r})$ the delayed arguments, $z = \alpha\gamma_p + \gamma_a$, $(\bar{\eta}, \bar{\beta}) = (\eta, \beta) \sqrt{1 + \alpha^2}$ with α the Henry's linewidth enhancement factor. If not otherwise stated, the parameters are $\alpha = 2$, $\gamma_a = 0$, $\gamma_p/\pi = 4.8$ GHz, $\eta/\pi = 8.68$ GHz, $\beta/\pi = 6.75$ GHz, $\tau_f = 3.3$ ns and $\tau_r = 3.5$ ns. The X and Y components of the intensity read

$$I_x = I_0 \cos^2(\Phi/2) \quad , \quad I_y = I_0 \sin^2(\Phi/2). \quad (3)$$

Figure 2(b,c) shows that, in each polarization, the main pulse is followed by a small inverted kink after a time $\Delta\tau = \tau_r - \tau_f$. This echo is the signature of the nonlocal coupling induced by the additional delay τ_r . It bears some similarity with the interaction between temporal LSs in injected Kerr fibers mediated by sound-waves [47], although here the effect is fully controllable and, as it

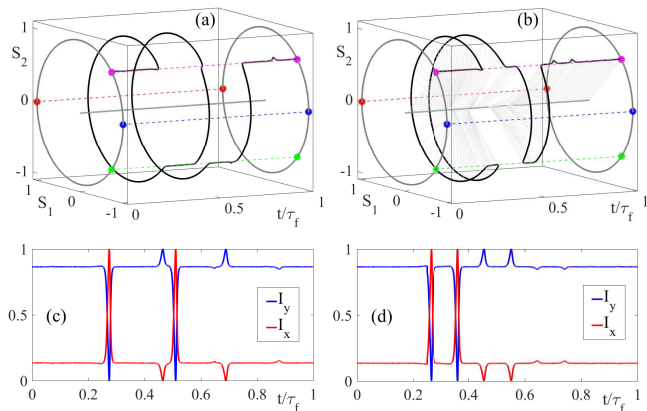


Figure 3. Numerical integration of Eq. (2). Evolution of the Stokes parameters (S_1, S_2) and intensities (I_x, I_y) in the cases of a covalent (a,c) and catenane (b,d) molecule. Pure emission along the X and Y directions correspond to the red and blue lines with $(S_1, S_2) = (1, 0)$ and $(S_1, S_2) = (-1, 0)$, respectively, while the steady state of Eq. 2 Φ_s is depicted in pink while the green line represents $-\Phi_s$.

will be shown below, it can be used to tune the interaction between LSs. These nonlocal echos create binding forces and allow the existence of LS molecules whose separation between elements is precisely $\Delta\tau$, as illustrated in Fig. 1b) and demonstrated in [42]. The structure of a typical covalent molecule is depicted in terms of the Stokes parameters and the polarization resolved intensities in Fig. 3a,c). Each localized state is composed by a large polarization kink for Φ followed by their nonlocal echo at $\Delta\tau$. The second LS is linked to the first via its echo, such that the bonding distance is $\Delta\tau$.

As illustrated in Fig. 1, when $\Delta\tau$ is sufficiently large with respect to the pulse size, a new kind of molecule of interlaced LSs can be observed where the second LS is trapped between the first LS and its echo. This molecule of nested LSs is represented in Fig. 3d) as a function of the polarization resolved intensities and in Fig. 3b) in terms of the Stokes parameters. After a large rotation corresponding to the primary peak of the first LS, the system performs the opposed movement in correspondence with the primary peak of the second LS, thus coming back to its original state. Similar but smaller kinks follow as the nonlocal echoes of the two LSs. Accordingly, Fig. 3b) evidences that this nested molecule has the additional property of being composed of a kink and an anti-kink, such that the total topological charge is zero.

Considering the LSs as periodic solutions of a high-dimensional dynamical system permitted us to perform the analysis of their Floquet multipliers. Floquet theory allows to study the linear stability of periodic solutions, see for instance [48]. The stability analysis performed in [42] confirmed that the covalent molecule in Fig. 3a,c) possesses a single neutral mode corresponding to the translation invariance of the whole molecule. The results of a similar analysis applied to the nested

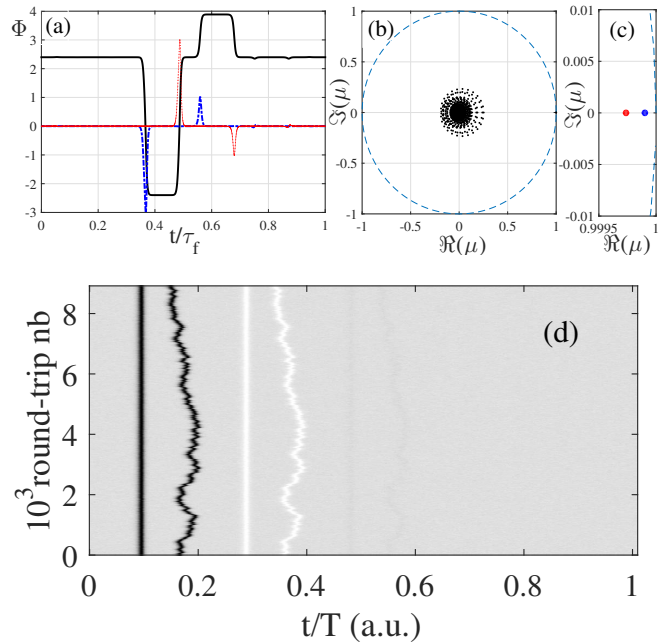


Figure 4. Numerical analysis of the catenane molecule in Fig. 3b,d). (a) Temporal profile (black) and the associated neutral eigenvectors (dotted blue and dash-dotted red). (b) Floquet multipliers μ and (c) zoom around $\mu = 1$ where one distinguishes two quasi-degenerate multipliers. (d) Space-time diagram of I_y in presence of additive white noise of amplitude $\xi = 3 \times 10^{-2}$. The position of each LS is given by the strong intensity dip followed by the smaller intensity peak echoing at $\Delta\tau$. The motion of the two intensity dips (dark peaks), mimicked by the corresponding echoes (white peaks), is completely uncorrelated, thus evidencing the local independence of the two LSs. The intensity of I_y grows from black to white.

molecule in Fig. 3b,d) are summarized in Fig. 4. The temporal profile of the solution over which we performed the stability analysis is depicted in Fig. 4a) and one notices in Fig. 4b) not one but *two* quasi-degenerate Floquet multipliers close to $\mu = 1$. We also show in Fig. 4a) the eigenvectors associated to these *two* neutral modes. One can easily identify them with the temporal derivatives of the kink and of the anti-kink composing the nested molecule, which allows for their individual translation. The residual interactions between LSs, which are always present if their separation is finite, renormalize the Floquet multipliers and explain their small deviation with respect to unity. In the limit $(\tau_f, \tau_r) \rightarrow (\infty, \infty)$ we find numerically that they converge to $\mu = 1$. In other words our *local* analysis shows that the two LSs composing the molecule are indeed locally independent. However, it fails to show their global dependence for which the consideration of the whole temporal profile is needed. The local independence of the LSs forming the bound state shown in Fig. 3b,d) contrasts with the rigid behavior of the components of the molecule shown in Fig. 3a,c). It also justifies our heuristic description of the molecule described

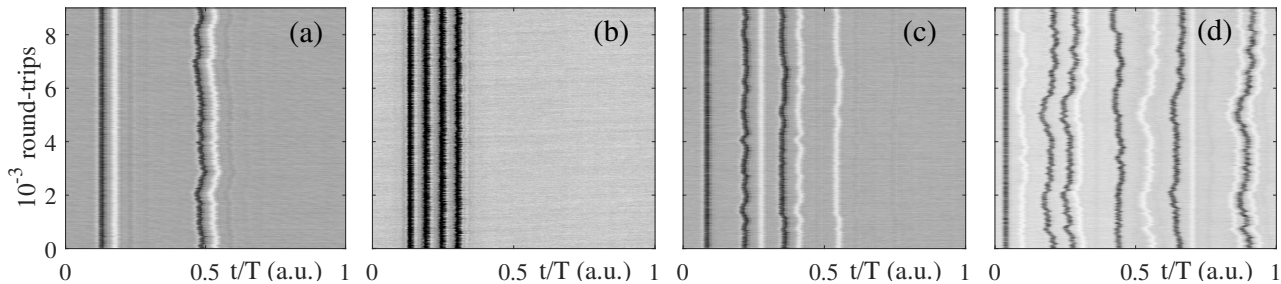


Figure 5. Experimental space-time diagrams taking the first LS as a time reference for visually enhancing the relative motion of other LSs. (a) two independent LSs, $\tau_r = \tau_f + 0.68$ ns. (b) covalent molecule with $\tau_r = \tau_f + 0.33$ ns and where the binding occurs via the interaction with the nonlocal echo (drown inside the large intensity dip). (b,c) Two different cases of catenane molecules with (c) $\tau_r = 2.3$ ns and (d) $\tau_r = 7.1$ ns. The intensity of I_y grows from black to white. Common parameters are $\tau_f = 10.8$ ns and $J = 10J_{th}$.

in Fig. 1c) as interlaced rings.

This evidence can be further supported by analyzing the motion of the structure represented in Fig. 3b,d) over many round-trips in presence of noise. As independent LSs and LS molecules coexist for the same parameter values, they can only be discriminated experimentally by observing their evolution on long timescales. While independent LSs exhibit uncorrelated random walks under the action of noise present in the system, LSs forming covalent molecules behave as a unique rigid body, see for instance Fig. 3a,b) in [42]. The stochastic evolution of the molecule described in Fig. 3b,d) is shown in Fig. 4d) by using a spatio-temporal diagram where the time trace for the polarization resolved intensity I_y is folded over itself at each period $T \simeq \tau_f$. Because we are plotting the intensity along the Y direction I_y , the LS main pulse corresponds to a dip (D) while the echo corresponds to small peak (P) at $\Delta\tau$ from D. In order to help visualizing the fluctuations of the distance between the molecule components, we have represented the LS evolution in the reference frame where the first LS remains static. As a consequence, while Fig. 4d) does not provide any information anymore regarding the random walk of the first LS, but it magnifies the evolution of relative distance between the two LSs. It also shows that, despite the fact that the two LSs can drift one respect to the other, the distance between them remains bounded and the main kink of the second LS is always caught between the main kink of the first LS and its echo. Also, this representation allows to distinguish between two elements catenanes and two independent LSs. The signature of the first corresponds to two dips (D) followed by two peaks (P), i.e. DDPP in Fig. 4d), while two independent LSs would correspond to DPDP.

Our theoretical predictions of the existence of catenane molecules are supported by experimental observations. A wealth of these molecule states has been observed in the experiment using the setup described in Fig. 2a), and they all coexist for the same parameter values. Some

examples are illustrated in Fig. 5. Besides two independent LSs in Fig. 5a), we represent in Fig. 5b) a standard covalent molecule found for small values of $\Delta\tau$, where the binding occurs via the nonlocal echo, which corresponds to the situation depicted in Fig. 1b). For larger values of $\Delta\tau$, and besides the simplest catenane corresponding to DDPP (not shown) we depict in Fig. 5c) a situation where three LSs are interlaced, giving the structures DDPDPP. Their local independence can be deduced from their relative uncorrelated motion, similar to that of independent LSs as depicted in Fig. 5a). Counting from left to right, we note that LS₂ is interlaced with LS₁, while LS₃ is interlaced with LS₂. A more complex catenane of 6 elements is shown in Fig. 5d). Here, two elements (LS₂ and LS₃) are very close to each other and their echoes trap a distant element (LS₆) driving its diffusion, thus evidencing the binding forces induced by the echo at the source of catenane molecules.

In conclusion, we described how the presence of a pointwise nonlocality in an extended system can give rise to a new kind of molecule of LSs whose elements are simultaneously locally independent and globally locked. Owing to the strong link between spatially extended and delayed systems, we have analyzed the implementation of pointwise nonlocality using a VCSEL enclosed in a double external cavity. The experimental signature of the optical catenane is found to closely match our predictions. We note that other TDSs capable of generating LSs as in [39, 40], would yield similar catenanes molecules.

ACKNOWLEDGMENTS

J.J. acknowledges financial support project COMBINA (TEC2015-65212-C3-3-P MINECO/FEDER UE) and the Ramón y Cajal fellowship. M.M and M.G. acknowledge the Universitat de les Illes Balears for funding a stay where part of this work was developed.

- [1] A. M. Turing. The chemical basis of morphogenesis. *Philos. Trans. R. Soc London*, 237:37, 1952.
- [2] J. Wu, R. Keolian, and I. Rudnick. Observation of a nonpropagating hydrodynamic soliton. *Phys. Rev. Lett.*, 52:1421–1424, Apr 1984.
- [3] E. Moses, J. Fineberg, and V. Steinberg. Multistability and confined traveling-wave patterns in a convecting binary mixture. *Phys. Rev. A*, 35:2757–2760, Mar 1987.
- [4] F. J. Niedernostheide, M. Arps, R. Dohmen, H. Willebrand, and H. G. Purwins. Spatial and spatio-temporal patterns in pnpn semiconductor devices. *physica status solidi (b)*, 172(1):249–266, 1992.
- [5] P. B. Umbanhowar, F. Melo, and H. L. Swinney. Localized excitations in a vertically vibrated granular layer. *Nature*, (382):793–796, 1996.
- [6] Yuri A. Astrov and H.G. Purwins. Plasma spots in a gas discharge system: birth, scattering and formation of molecules. *Physics Letters A*, 283(5-6):349 – 354, 2001.
- [7] N. N. Rosanov and G. V. Khodova. Autosolitons in nonlinear interferometers. *Opt. Spectrosc.*, 65:449–450, 1988.
- [8] W. J. Firth and A. J. Scroggie. Optical bullet holes: Robust controllable localized states of a nonlinear cavity. *Phys. Rev. Lett.*, 76:1623–1626, Mar 1996.
- [9] M. Brambilla, L. A. Lugiato, F. Prati, L. Spinelli, and W. J. Firth. Spatial soliton pixels in semiconductor devices. *Phys. Rev. Lett.*, 79:2042–2045, 1997.
- [10] L.A. Lugiato. Introduction to the feature section on cavity solitons: An overview. *Quantum Electronics, IEEE Journal of*, 39(2):193–196, 2003.
- [11] S. Barland, J. R. Tredicce, M. Brambilla, L. A. Lugiato, S. Balle, M. Giudici, T. Maggipinto, L. Spinelli, G. Tissoni, T. Knödl, M. Miller, and R. Jäger. Cavity solitons as pixels in semiconductor microcavities. *Nature*, 419(6908):699–702, Oct 2002.
- [12] F. Leo, S. Coen, P. Kockaert, S.P. Gorza, P. Emplit, and M. Haelterman. Temporal cavity solitons in one-dimensional kerr media as bits in an all-optical buffer. *Nat Photon*, 4(7):471–476, Jul 2010.
- [13] P. Genevet, S. Barland, M. Giudici, and J. R. Tredicce. Cavity soliton laser based on mutually coupled semiconductor microresonators. *Phys. Rev. Lett.*, 101:123905, Sep 2008.
- [14] Y. Tanguy, T. Ackemann, W. J. Firth, and R. Jäger. Realization of a semiconductor-based cavity soliton laser. *Phys. Rev. Lett.*, 100:013907, Jan 2008.
- [15] T. Herr, V. Brasch, J. D. Jost, C. Y. Wang, N. M. Kondratiev, M. L. Gorodetsky, and T. J. Kippenberg. Temporal solitons in optical microresonators. *Nature Photonics*, 8(2):145–152, 2014.
- [16] N. N. Rosanov and G. V. Khodova. Diffractive autosolitons in nonlinear interferometers. *J. Opt. Soc. Am. B*, 7:1057–1065, 1990.
- [17] J. M. McSloy, W. J. Firth, G. K. Harkness, and G.-L. Oppo. Computationally determined existence and stability of transverse structures. ii. multi-peaked cavity solitons. *Phys. Rev. E*, 66:046606, Oct 2002.
- [18] H. L. Frisch and E. Wasserman. Chemical topology. *Journal of the American Chemical Society*, 83(18):3789–3795, 1961.
- [19] P. L. Ramazza, S. Ducci, and F. T. Arecchi. Optical diffraction-free patterns induced by a discrete translational transport. *Phys. Rev. Lett.*, 81:4128–4131, Nov 1998.
- [20] Francesco Papoff and Roberta Zambrini. Convective instability induced by nonlocality in nonlinear diffusive systems. *Phys. Rev. Lett.*, 94:243903, Jun 2005.
- [21] Roberta Zambrini and Francesco Papoff. Signal amplification and control in optical cavities with off-axis feedback. *Phys. Rev. Lett.*, 99:063907, Aug 2007.
- [22] S. Residori, T. Nagaya, and A. Petrossian. Optical localised structures and their dynamics. *EPL (Europhysics Letters)*, 63(4):531, 2003.
- [23] C. Fernandez-Oto, M. G. Clerc, D. Escaff, and M. Tlidi. Strong nonlocal coupling stabilizes localized structures: An analysis based on front dynamics. *Phys. Rev. Lett.*, 110:174101, Apr 2013.
- [24] M. Tlidi, C. Fernandez-Oto, M. G. Clerc, D. Escaff, and P. Kockaert. Localized plateau beam resulting from strong nonlocal coupling in a cavity filled by metamaterials and liquid-crystal cells. *Phys. Rev. A*, 92:053838, Nov 2015.
- [25] D. Escaff, C. Fernandez-Oto, M. G. Clerc, and M. Tlidi. Localized vegetation patterns, fairy circles, and localized patches in arid landscapes. *Phys. Rev. E*, 91:022924, Feb 2015.
- [26] W. Firth, L. Columbo, and A. Scroggie. Proposed resolution of theory-experiment discrepancy in homoclinic snaking. *Phys. Rev. Lett.*, 99:104503, Sep 2007.
- [27] O. Thual and S. Fauve. Localized structures generated by subcritical instabilities. *J. Phys. France*, 49:1829–1833, 1988.
- [28] S. Fauve and O. Thual. Solitary waves generated by subcritical instabilities in dissipative systems. *Phys. Rev. Lett.*, 64:282–284, Jan 1990.
- [29] F. T. Arecchi, G. Giacomelli, A. Lapucci, and R. Meucci. Two-dimensional representation of a delayed dynamical system. *Phys. Rev. A*, 45:R4225–R4228, Apr 1992.
- [30] G. Giacomelli and A. Politi. Relationship between delayed and spatially extended dynamical systems. *Phys. Rev. Lett.*, 76:2686–2689, Apr 1996.
- [31] S.A. Kashchenko. The Ginzburg-Landau equation as a normal form for a second-order difference-differential equation with a large delay. *Comput. Math. Math. Phys.*, 38(3):1, 1998.
- [32] Svetlana V. Gurevich. Dynamics of localized structures in reaction-diffusion systems induced by delayed feedback. *Phys. Rev. E*, 87:052922, May 2013.
- [33] Laurent Larger, Bogdan Penkovsky, and Yuri Maistrenko. Virtual chimera states for delayed-feedback systems. *Phys. Rev. Lett.*, 111:054103, Aug 2013.
- [34] Giovanni Giacomelli, Francesco Marino, Michael A. Zaks, and Serhiy Yanchuk. Coarsening in a bistable system with long-delayed feedback. *EPL (Europhysics Letters)*, 99(5):58005, 2012.
- [35] Giovanni Giacomelli, Francesco Marino, Michael A. Zaks, and Serhiy Yanchuk. Nucleation in bistable dynamical systems with long delay. *Phys. Rev. E*, 88:062920, Dec 2013.
- [36] Francesco Marino, Giovanni Giacomelli, and Stephane Barland. Front pinning and localized states analogues in long-delayed bistable systems. *Phys. Rev. Lett.*, 112:103901, Mar 2014.

- [37] J. Javaloyes, T. Ackemann, and A. Hurtado. Arrest of domain coarsening via anti-periodic regimes in delay systems. *Phys. Rev. Lett.*, 115:223901, Nov 2015.
- [38] Serhiy Yanchuk and Giovanni Giacomelli. Pattern formation in systems with multiple delayed feedbacks. *Phys. Rev. Lett.*, 112:174103, May 2014.
- [39] M. Marconi, J. Javaloyes, S. Balle, and M. Giudici. How lasing localized structures evolve out of passive mode locking. *Phys. Rev. Lett.*, 112:223901, Jun 2014.
- [40] B. Garbin, J. Javaloyes, G. Tissoni, and S. Barland. Topological solitons as addressable phase bits in a driven laser. *Nat. Com.*, 6, 2015.
- [41] B. Romeira, R. Avó, José M. L. Figueiredo, S. Barland, and J. Javaloyes. Regenerative memory in time-delayed neuromorphic photonic resonators. *Scientific Reports*, 6:19510 EP –, Jan 2016. Article.
- [42] M. Marconi, J. Javaloyes, S. Barland, S. Balle, and M. Giudici. Vectorial dissipative solitons in vertical-cavity surface-emitting lasers with delays. *Nature Photonics*, 2015.
- [43] J. Javaloyes. Cavity light bullets in passively mode-locked semiconductor lasers. *Phys. Rev. Lett.*, 116:043901, Jan 2016.
- [44] Serhiy Yanchuk and Giovanni Giacomelli. Spatio-temporal phenomena in complex systems with time delays. *Journal of Physics A: Mathematical and Theoretical*, 50(10):103001, 2017.
- [45] M. San Miguel, Q. Feng, and J. V. Moloney. Light-polarization dynamics in surface-emitting semiconductor lasers. *Physical Review A (Atomic, Molecular, and Optical Physics)*, 52(2):1728–1739, 1995.
- [46] J. Javaloyes, M. Marconi, and M. Giudici. Phase dynamics in vertical-cavity surface-emitting lasers with delayed optical feedback and cross-polarized reinjection. *Phys. Rev. A*, 90:023838, Aug 2014.
- [47] J. K. Jang, M. Erkintalo, S. G. Murdoch, and S. Coen. Ultraweak long-range interactions of solitons observed over astronomical distances. *Nat Photon*, 7(8):657–663, Aug 2013. Article.
- [48] Christopher A. Klausmeier. Floquet theory: a useful tool for understanding nonequilibrium dynamics. *Theoretical Ecology*, 1(3):153–161, 2008.